Geotechnical Engineering in the XXI Century: Lessons learned and future challenges
N.P. López-Acosta et al. (Eds.)

doi:10.3233/STAL190081

Geomechanical Characterization of MICP-Treated Soils

Ronak MEHRABI[a] and Kamelia ATEFI-MONFARED [a,1]
[a]*Dept. of Civil, Structural, and Environmental Engineering, University at Buffalo*

Abstract. Microbial induced calcite precipitation (MICP) process has proven to play an active role in modification of in-situ porosity, permeability, and improvement of strength and stiffness of granular unconsolidated soils. Characterization of the resulting alterations in the bio-enhanced porous matrix remains to be a critical gap. This paper is aimed at modeling biological clogging and the resulting geomechanical alterations in a sand sample through a novel numerical scheme. A new tightly coupled numerical model is developed to assess the spatiotemporal geomechanical variations in an unconsolidated sand subjected to MICP treatment. The progress of calcite precipitation is implemented into the model using the Monod-type kinetics rate formulation. The modification in stiffness parameters is predicted using a cementation theory based on time-dependent porosity reduction under cement deposition in the soil matrix.

Keywords. Microbial induced calcite precipitation, Coupled processes, Numerical model, bio-poroelastic processes.

1. Introduction

Microbial induced calcite precipitation (MICP) – the most researched bio-inspired soil cementation process – involves hydrolysis of urea catalyzed by means of certain microorganisms (i.e. Sporosarcina pasteurii), producing calcite or calcium carbonate ($CaCO_3$) precipitate. The latter either bonds soil grains at their contacts or occupies void spaces within the target soil matrix. MICP-treatment impacts permeability, stiffness, compressibility, and shear strength of the treated layer [1]. The ability of MICP-treatment to improve compressive strength, shear strength, and stiffness, particularly in granular soils (i.e., sands and gravels), has been explored through laboratory column tests, triaxle tests, unconfined compressive tests, and in a few large scale experiments (e.g. [2, 3]).

Analytical analyses, developed to forecast the extent of improvement in engineering properties of soils, treated by traditional non-bio-inspired methods, can be fairly used to model bio-cemented soils. The increase in strength and stiffness and the reduction of porosity observed in the MICP-treated samples resembles cases where Portland cement, gypsum, and epoxy were adopted for soil enhancement [4,5]. Consequently, the available theoretical and analytical models can be adopted and implemented in bio-mediated research area to simulate soil laboratory samples using advanced computational resources.

Numerical modeling is an effective computational technique for assessing the upscaling of bio-cementation. Discrete element method (DEM) is perhaps the most

[1] Corresponding Author; E-mail: kameliam@buffalo.edu.

suitable technique to explore the behavior of MICP-cemented sands [6,7]. The micro-scale mechanics provide important insight into the behavior of a granular material, however, the method has not yet been widely implemented in practical engineering. A major drawback of DEM is its computational requirement where large number of particles are needed to reasonably assess the involved coupled processes – specifically for field scale implementation – making the program impractical. It would thus be more effective to adopt continuum-based numerical analyses, since the geometry of the mechanical system remains reserved, decreasing the simulation time and accuracy for modeling bio-cementation in porous strata.

This paper presents a novel tightly coupled numerical scheme for simulating MICP-cementation via bio-stimulation (enrichment of native bacteria in soil) in sands through adopting the continuum-based FLAC3D software [8]. The progress of calcite precipitation is implemented in the model using Monod-typerate formulation [9], the widely adopted mathematical expression for describing specific growth/reaction rate as function of the concentration of a limiting substrate. The changes in porosity due to pore-filling calcium carbonate is estimated by an exact analytical solution derived by [10]. Improvement in sand stiffness parameters is predicted using the constant-cement theory proposed by [5], which considers the effect of time-dependent porosity reduction on the values of elastic moduli of the cemented matrix.

2. Mathematical background

2.1. Bio-cement assessment

Engineered promotion of calcium carbonate precipitation in soils is initiated by injecting a cementation solution (urea ($CO(NH_2)_2$) and calcium chloride ($CaCl_2$)) into locations where strengthening is required. Bio-cementation via calcium carbonate precipitation can be applied in variety of situations without much disturbance of subsoil. However, the successful application requires the understanding of the involved processes and choosing the right process parameters including concentrations of species (e.g. urea, calcium chloride). Similarly, analyzing and describing bio-cementation process through mathematical modeling requires that all the process parameters be considered for the model to be precise and predictive of the location and level of the precipitated cement.

During MICP-treatment of soil, the porosity is time dependent, i.e., porosity and permeability gradually decrease. The induced changes in porosity modifies the flow regime, soil density and stiffness parameters. The biological assessment in our proposed model considers overtime accumulation of calcium carbonate and time-dependent decrease in porosity, using the bio-grout model by [10]. In the latter model, the Monod-type reaction rate for calcite precipitation follows the formulation of Eq. (1) [10]:

$$r_{reaction} = v_{max} \frac{C^{urea}}{K_m + C^{urea}} \left(1 - \frac{t}{t_{max}}\right) \qquad if \quad 0 \le t \le t_{max} \tag{1}$$

where v_{max} presents the maximum reaction rate and is constant since the distribution of bacteria is assumed to be homogenous. K_m stands for half saturation constant and C^{urea} is the concentration of urea. The Eq. (1) assumes a linear decay of microorganisms, meaning that during t_{max} (sec), the reaction rate decreases from v_{max} to 0.

To predict the changes in porosity while the pore volume is being filled with calcium carbonate, [10] presented the Eq. (2) for porosity, n, as a function of time, t:

$$n(t) = n_0 \exp\left\{-\frac{m_{CaCa_3}}{\rho_{CaCa_3}} v_{max} \frac{C^{urea}}{K_m + C^{urea}}\left(t - \frac{t^2}{2t_{max}}\right)\right\} \quad (2)$$

Similarly, the Eq. (3) can be used for calculation of calcium carbonate concentration as function of time:

$$C^{CaCa_3}(t) = C^{CaCa_3}(0) + \rho_{CaCa_3} n_0 \left\{1 - \exp\left\{-\frac{m_{CaCa_3}}{\rho_{CaCa_3}} v_{max} \frac{C^{urea}}{K_m + C^{urea}}\left(t - \frac{t^2}{2t_{max}}\right)\right\}\right\} \quad (3)$$

The parameter n_0 represents the initial porosity and m_{CaCa_3}, C^{CaCa_3}, and ρ_{CaCa_3} are the molar mass, concentration, and density of calcium carbonate, respectively.

The analytically derived Eqs. (2) and (3) can be used to calculate porosity reduction at places with constant urea concentrations over time. However, the distribution of urea concentration is not uniform, being higher near the injection area. Hence, we solved, in an uncoupled manner, the formulation for distribution of urea concentration at small computational time steps and implement the obtained values in Eqs. (2) and (3). Assuming continuous source of urea at injection point (top of the simulated model), the evolution of urea concentration is derived by analytically solving advection-diffusion equation in one dimension as Eq. (4):

$$C^{urea}(x,t) = (\frac{C_0^{urea}}{2})\left[\exp\left(\frac{uz}{D}\right)\operatorname{erfc}\left(\frac{z+ut}{\sqrt{4Dt}}\right) + \operatorname{erfc}\left(\frac{z-ut}{\sqrt{4Dt}}\right)\right] \quad (4)$$

where C_0^{urea} is the initial concentration of urea and D being its diffusion coefficient. z is the distance from injection point along the length of the simulated model and u is the average flow velocity.

The time dependent formulations for porosity and concentration of urea were implemented in FLAC3D [8] using the *Fish* programming language. Permeability and elastic moduli are set to be evolved as functions of time-variable porosity over small time steps. The decrease in permeability is calculated using Kozney-Carman-type equation [11]:

$$\frac{K}{K_0} = (\frac{n - n_{crit}}{n_0 - n_{crit}})^3 \quad (5)$$

where K and K_0 are the current and initial permeability, respectively, and n_{crit} is the critical porosity at which permeability is 0. We assume $n_{crit} = 0$.

2.2. Cementation theory

The evolution of strength and stiffness of sand from biological calcite precipitation can be reasonably estimated, as function of cementation, through theoretical analysis developed for traditional non-bio-based treatments [1]. The developed theoretical and empirical models forecast the seismic responses in terms of several geological characteristics (e.g. porosity, clay or other cement content, saturation) of rocks/soils [12]. These models and predictions help us better understand rock/soil properties beyond elasticity [12].

It has been established that elastic moduli and porosity are connected approximately in a linear manner. [4] introduced two theoretical models for high porosity sand to track the changes in elastic moduli when the porosity is altered by cement deposition: contact-cement model and friable-sand model.

The contact-cement model assumes that the initial reduction of porosity is due to deposition of cement in two schemes: either uniformly coating the grain surface, or forming a bridge at grain contacts. The contact-cement model captures dramatic increases in the sand's elastic moduli with even minuscule reductions in porosity. Hence, even a tiny amount of cement is load bearing and significantly increases the stiffness of granular matrix. The contact-cement theory suggests the effective bulk (K_{eff}), and shear (G_{eff}) moduli of a random pack of identical spherical grains with elastic cement at their contacts depend on the amount/properties of the cement and grains as given by Eqs. (6) and (7). The cementing agent may be quartz, calcite or clay.

$$K_{eff} = \left(\frac{1}{6}\right) m(1 - n_0) M_c S_n \tag{6}$$

$$G_{eff} = \left(\frac{3}{5}\right) K_{eff} + \left(\frac{3}{20}\right) m(1 - n_0) G_c S_\tau \tag{7}$$

where M_c and G_c are the compressional and shear moduli of the cement, respectively. S_n and S_τ are proportional to normal and shear stiffness of a cemented two-grain combination. $m = 9$ is the average number of contacts per grain. The amount of contact cement can be expressed through ratio α of the radius of cement layer to the grain radius. When all the cement is deposited at grain contacts then the α can be calculated as:

$$\alpha = 2\left(\frac{n_0 - n}{3m(1 - n_0)}\right)^{0.25} \tag{8}$$

More details of the contact-cement theory can be found in [4].

The second model by [4], known as friable-sand model, considers the effect of porosity reduction on elastic parameters due to deposition of cement in the pore spaces, away from grain contacts. Apparently, this part of deposited cement has moderate effects on increasing the stiffness of cemented media, compared to contact cement deposition.

Avseth et al (2000) stablished the new constant-cement model as combination of contact-cement and friable sand model [5]. Based on this model, the initial reduction in porosity, from n_0 to n_b is due to contact cement deposition. Later, further reduction in porosity occurs by non-contact pore-filling cement deposition. Eqs. (9) and (10) calculate the dry-bulk and dry-shear moduli at porosities smaller than n_b, based on friable sand model.

$$K_{dry} = \left(\frac{\left(\frac{n}{n_b}\right)}{K_b + \left(\frac{4}{3}\right) G_b} + \frac{\left(1 - \frac{n}{n_b}\right)}{K_s + \left(\frac{4}{3}\right) G_b} \right)^{-1} - \left(\frac{4}{3}\right) G_b \tag{9}$$

$$G_{dry} = \left(\frac{\left(\frac{n}{n_b}\right)}{G_b + A} + \frac{\left(1 - \frac{n}{n_b}\right)}{G_s + A} \right)^{-1} - A\,, \quad A = \left(\frac{G_b}{6}\right)\left(\frac{9K_b + 8G_b}{K_b + 2G_b}\right) \tag{10}$$

where K_b and G_b are dry bulk and shear moduli at porosity n_b, respectively, calculated through Eqs. (6) and (7); K_s and G_s are bulk and shear moduli of the mineral phase, respectively. The effect of pore fluid on elastic moduli can be accounted by Gassmann's theory [13].

3. Numerical simulation and results

A numerical model has been developed using FLAC3D to replicate biologically induced clogging and cementation in sand, through implementing the abovementioned mathematical formulation. We aim to illustrate the effect of overtime calcium carbonate cementation on permeability, porosity, elastic moduli and in situ flow regime. A schematic of the problem is presented in Figure 1. The model resembles a typical cylindrical soil column (72mm internal diameter, 150 mm high), in fully water-saturated conditions. The material properties chosen for the soil grains are similar to those of quartz sand. With respect to the elastic cement, the properties of calcite have been considered.

Table 1 present the input values for the simulations, mainly taken from the published literature (e.g. [10]). Initial conditions were set to achieve static equilibrium prior to introducing cementation. The computational time step in FLAC3D was scaled to present 1 hour of bio-cementation process. This modification of time step in FLAC3D does not affect the final mechanical behavior observed in treated sand. To reduce the initial dramatic rise in sand's elastic moduli with small reduction in porosity, n_b was selected to be close to the initial porosity, n_0. n_b should be calibrated against laboratory data and, if available, microscopic images, to best represent the amount of cementation.

Table 1. Material properties of sand and values for biological assessment adopted for numerical simulation.

Properties	Units	Values
Initial porosity, n_0	-	0.425
Initial permeability, k_{perm}	m^2/(pa.sec)	1.85×10^{-7}
Initial bulk modulus of sand pack	MPa	41.6
Initial shear modulus of sand pack	MPa	19
Friction angle	degree	30
Shear modulus of grains (quartz sand), K_s	GPa	37
Shear modulus of grains (quartz sand), G_s	GPa	44
Bulk modulus of cement (calcite), K_c	GPa	77
Shear modulus of cement (calcite), G_c	GPa	32
Injection rate	m/hr	1×10^{-5}
Initial concentration of urea, C_0^{urea}	kmol/m^3	0.33
Half saturation constant, K_m	kmol/m^3	0.01
Density of calcium carbonate, ρ_{CaC03}	kg/m^3	2710
Molar mass of calcium carbonate, m_{CaCO3}	kg/kmol	100.1
Diffusion coefficient of urea, D	m^2/s	1×10^{-9}
Maximum reaction rate, v_{max}	kmol/m^3/s	9×10^{-5}
Maximum time of reaction, t_{max}	hr	170

Contours of porosity, permeability, pore pressure, compression and shear moduli are also depicted in Figure 1 at t = 15 hours, the maximum time of MICP treatment. As shown, the bio-cementation process affects several properties in the treated sand. The precipitation of calcium carbonate at an initial porosity of 0.425 caused a decrease in the porosity up to value of 0.359 (about 15% decrease), after 15 hours of constant injection of the cementation solution. The resultant reduction in porosity is highest near the injection point, where the concentration of urea, modeled using Eq. (4), is the maximum. Such reduction in porosity resulted in a 39% decrease in permeability. In response to this decrease in permeability, the pressures increased, to maintain a constant flow rate.

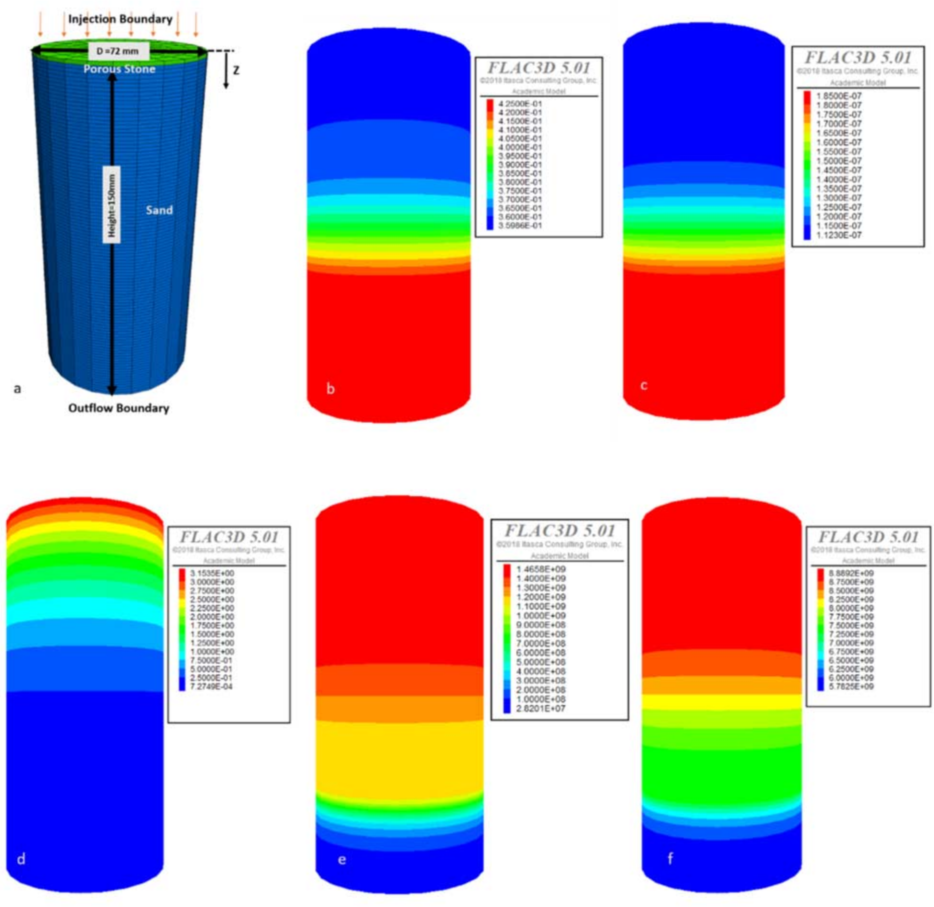

Figure 1. (a) Configuration and boundary condition of the simulated soil sample, and contours of (b) porosity, (c) permeability ($m^2/(pa.sec)$), (d) pore water pressure (Pa), (e) shear modulus (Pa), and (f) compression modulus (Pa).

From Figure 1, the maximum increase in compression and shear moduli has happened at the top of the sample where more calcium carbonate has precipitated. The amount of precipitated calcium carbonate, as shown in Figure 2, increases in time, in an approximate linear manner, for the duration of the treatment. Using Eq. (3), the maximum content of precipitated calcite is calculated to be 180 kg/m^3 (Figure 2), sufficient to attain a desirable strong soil in most applications [10].

Shear modulus alterations against time and porosity are plotted in Figure 3. The high-sloped part of the graphs represents the contact cement deposition. Next, further cement deposition occurs in pore spaces, resulting in gradual effects on evolution of shear modulus. The final shear modulus is about 77 times that of the initial value. [14] has reported a 55 times increase in a heavily cemented specimen. It should be noted that the presented model has been created under several assumptions. Using the current model, the captured modifications in permeability and stiffness parameters may not exactly reflect the real data unless being validated using laboratory experiments.

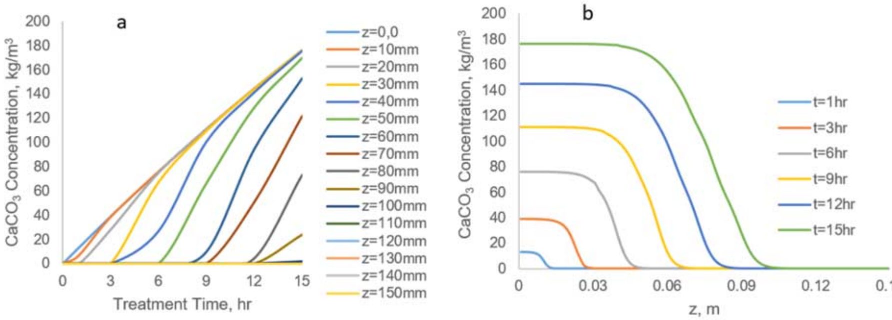

Figure 2. Calcium carbonate concentration; (a) overtime precipitation, (b) distribution.

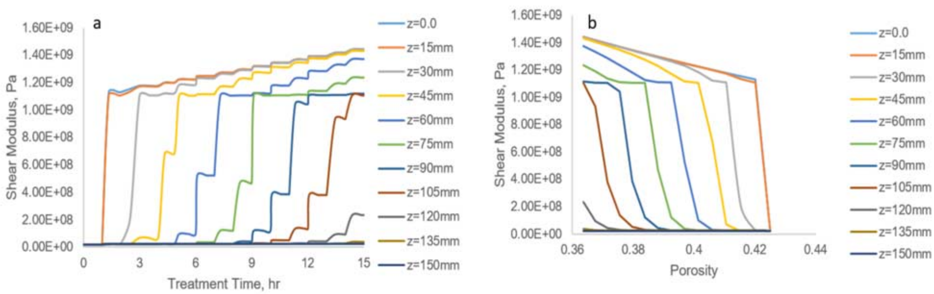

Figure 3. Shear modulus; (a) overtime increase, (b) versus porosity reduction.

4. Concluding remarks

The presented study highlights the feasibility of a continuum-based numerical resource to be able to capture the macro-scale mechanical behavior of sandy soils based on the evolution of calcium carbonate precipitation at granular scale.

The most influencing factor affecting the macroscale geotechnical behavior is the amount and the location of precipitated calcite in the granular soil matrix. As discussed earlier, the contact cement deposition dramatically increases the stiffness, compared to the case where cement is deposited in voids of soil matrix.

It should be emphasized that boundary conditions for pressure, injection flow, urea concentration, and reaction and input parameters might be case specific and unique to the physical experiments, thus should be validated versus physical experiments. Further research is ongoing for calibrating the developed model against real laboratory data.

References

[1] DeJong, J. T., Mortensen, B. M., Martinez, B. C., & Nelson, D. C. (2010). Bio-mediated soil improvement. Ecological Engineering, 36(2), 197-210.
[2] DeJong, J. T., Fritzges, M. B., & Nüsslein, K. (2006). Microbially induced cementation to control sand response to undrained shear. Journal of Geotechnical and Geoenvironmental engineering, 132(11), 1381-1392.
[3] Gomez, M. G. (2017). Up-scaling of Bio-Cementation Soil Improvement Using Native Soil Microorganisms: University of California, Davis.
[4] Dvorkin, J., & Nur, A. (1996). Elasticity of high-porosity sandstones: Theory for two North Sea data sets. Geophysics, 61(5), 1363-1370.
[5] Avseth, P., Dvorkin, J., Mavko, G., & Rykkje, J. (2000). Rock physics diagnostic of North Sea sands: Link between microstructure and seismic properties. Geophysical Research Letters, 27(17), 2761-2764.
[6] Feng, K., Montoya, B., & Evans, T. (2017). Discrete element method simulations of bio-cemented sands. Computers and Geotechnics, 85, 139-150.
[7] Akimana, R. M., Bista, H., Seo, Y., Li, L., Howard, L. J., Dewoolkar, M. M., & Hu, L.-B. Multi-Scale Experimental and Numerical Study of Microbially-Induced Calcite Precipitation in Sandy Soils: Preliminary Evidence and Observations. In Geo-China 2016 (pp. 77-84).
[8] Itasca Consulting Group, Inc. (2018) FLAC3D — Fast Lagrangian Analysis of Continua in Three Dimensions, Ver. 5.01. Minneapolis: Itasca.
[9] Monod J. (1949). The growth of bacterial cultures. Annual Reviews in Microbiology, 3(1), 371-394
[10] Van Wijngaarden, W., Vermolen, F., Van Meurs, G., & Vuik, C. (2011). Modelling biogrout: a new ground improvement method based on microbial-induced carbonate precipitation. Transport in porous media, 87(2), 397-420.
[11] Ebigbo, A., Phillips, A., Gerlach, R., Helmig, R., Cunningham, A. B., Class, H., & Spangler, L. H. (2012). Darcy-scale modeling of microbially induced carbonate mineral precipitation in sand columns. Water Resources Research, 48(7).
[12] Avseth, P., Mukerji, T., Mavko, G., & Dvorkin, J. (2010). Rock-physics diagnostics of depositional texture, diagenetic alterations, and reservoir heterogeneity in high-porosity siliciclastic sediments and rocks—A review of selected models and suggested work flows. Geophysics, 75(5), 75A31-75A47.
[13] Gassmann, F. (1951). Elasticity of porous media. Vierteljahrsschrder Naturforschenden Gesselschaft, 96, 1-23.
[14] Montoya, B. M., & DeJong, J. T. (2015). Stress-strain behavior of sands cemented by microbially induced calcite precipitation. Journal of Geotechnical and Geoenvironmental Engineering, 141(6), 04015019.